High-efficiency channelrhodopsins for fast neuronal stimulation at low light levels

André Berndt[a,1], Philipp Schoenenberger[b,1], Joanna Mattis[c], Kay M. Tye[c], Karl Deisseroth[c], Peter Hegemann[a], and Thomas G. Oertner[b,2]

[a]Experimental Biophysics, Humboldt-Universität zu Berlin, D-10115 Berlin, Germany; [b]Friedrich Miescher Institute for Biomedical Research, CH-4058 Basel, Switzerland; and [c]Department of Bioengineering, Stanford University, Stanford, CA 94305

Edited by Roger A. Nicoll, University of California, San Francisco, CA, and approved March 28, 2011 (received for review November 16, 2010)

Channelrhodopsin-2 (ChR2) has become an indispensable tool in neuroscience, allowing precise induction of action potentials with short light pulses. A limiting factor for many optophysiological experiments is the relatively small photocurrent induced by ChR2. We screened a large number of ChR2 point mutants and discovered a dramatic increase in photocurrent amplitude after threonine-to-cysteine substitution at position 159. When we tested the T159C mutant in hippocampal pyramidal neurons, action potentials could be induced at very low light intensities, where currently available channelrhodopsins were unable to drive spiking. Biophysical characterization revealed that the kinetics of most ChR2 variants slows down considerably at depolarized membrane potentials. We show that the recently published E123T substitution abolishes this voltage sensitivity and speeds up channel kinetics. When we combined T159C with E123T, the resulting double mutant delivered fast photocurrents with large amplitudes and increased the precision of single action potential induction over a broad range of frequencies, suggesting it may become the standard for light-controlled activation of neurons.

hippocampus | optogenetics | photocycle | pyramidal cell | spike frequency

Optogenetic stimulation of neurons using Channelrhodopsin-2 (ChR2) has become a widely used tool in neuroscience. ChR2, a directly light-gated cation channel of the green algae *Chlamydomonas reinhardtii*, allows depolarizing and firing neurons with brief blue light pulses (1, 2). Because the single channel conductance of ChR2 is very small, high expression levels are required to fire neurons reliably. Over the last few years, techniques for ChR2 expression in neurons have been improved substantially. High expression levels can be obtained by expressing ChR2 under the control of strong promoters, for example, in virally transduced neurons. In mice, the combination of Cre-dependent viruses with specific Cre-expressing driver lines has enabled strong ChR2 expression in cell types where no specific strong promoters are known (3, 4). Despite these advanced expression strategies, reliable and well-timed action potential (AP) induction can still be difficult, especially at high stimulation frequencies or for in vivo experiments where local light intensities are low. Several engineered channelrhodopsins that address some of the current limitations have been reported. ChR2(H134R), carrying a single point mutation at position H134, generates larger photocurrents than wild-type (wt) ChR2, but slows down channel kinetics, which can interfere with the precision of single AP induction (5). The recently reported E123T ("ChETA") mutation speeds up channel kinetics but reduces photocurrent amplitudes (6). Combined with the H134R mutation, E123T produced photocurrents that nearly reached the amplitude of wt ChR2 currents while preserving favorable accelerated kinetics, enabling stimulation of fast spiking interneurons at up to 200 Hz (6). Pyramidal cells, because of their different K^+ channel complement, resist such high spike frequencies (7).

Finally, the bistable C128 variants have very-long-lived open channel states and therefore induce neuronal depolarization at very low light intensities (8). Because of their slow kinetics and strong light-dependent inactivation, however, bistable ChR2 variants are not suitable for long-term control of AP induction (9). To control AP firing in large neurons such as cortical pyramidal cells with high reliability and temporal precision even at high frequencies, mutants that can generate large photocurrents with rapid channel kinetics are required (10). Ideally, if such mutants did also work at low light intensities, stimulation through thick layers of tissue could become possible, obviating the need to implant optical fibers into the animal. Here we present two previously undescribed ChR2 variants that improve the reliability and versatility of optogenetic neuronal stimulation. ChR2(T159C), which we refer to as "ChR2-TC" or simply "TC," generates very large photocurrents and sensitizes neurons to very low light intensities. The E123T/T159C double mutant (ET/TC) enables reliable and sustained optical stimulation of hippocampal pyramidal neurons up to 60 Hz. Our biophysical analysis suggests that the fast and voltage-independent kinetics of ET/TC are responsible for the excellent performance at high frequencies.

Results

ChR2(T159C) Increases Photocurrent Amplitude in *Xenopus* Oocytes. The retinal binding pocket of ChR2 is conserved from other microbial opsins such as bacteriorhodopsin, of which high-resolution 3D structures are available (11). Using this structural homology as a guideline, we were able to target mutations specifically to the retinal binding pocket of ChR2, affecting channel properties such as ion selectivity, kinetics, and absorbed wavelengths. Point mutants were characterized in *Xenopus* oocytes, a well-established test system for the kinetic analysis of photocurrents. We screened >50 ChR2 mutants and found quite dramatic changes after amino acid substitutions at position T159, in close vicinity to the previously characterized C128 and D156 residues (Fig. 1*A*). Mutation of Thr-159 to Cys (TC) resulted in a dramatic increase of photocurrent amplitudes but, in contrast to mutations at the C128 and D156 positions, did not result in bistable behavior (Fig. 1*B*). Because ChR2(H134R) (or briefly, HR; ref. 5) has become a popular choice for neuronal stimulation, we included this mutant for comparison (green trace, Fig. 1*B*). We confirmed that the stationary current of HR in oocytes increased approximately three times compared with wt ChR2 (Fig. 1*C*). In the TC mutant, however, current amplitudes were >10 times larger compared with wt ChR2.

Large photocurrents are very desirable but are often accompanied by slower channel kinetics. We measured the time con-

Author contributions: A.B., P.S., K.D., P.H., and T.G.O. designed research; A.B., P.S., J.M., and K.M.T. performed research; A.B. and P.H. contributed new reagents/analytic tools; A.B., P.S., J.M., and K.M.T. analyzed data; and A.B., P.S., P.H., and T.G.O. wrote the paper.

The authors declare no conflict of interest.

This article is a PNAS Direct Submission.

[1]A.B. and P.S. contributed equally to this work.

[2]To whom correspondence should be addressed. E-mail: thomas.oertner@fmi.ch.

This article contains supporting information online at www.pnas.org/lookup/suppl/doi:10.1073/pnas.1017210108/-/DCSupplemental.

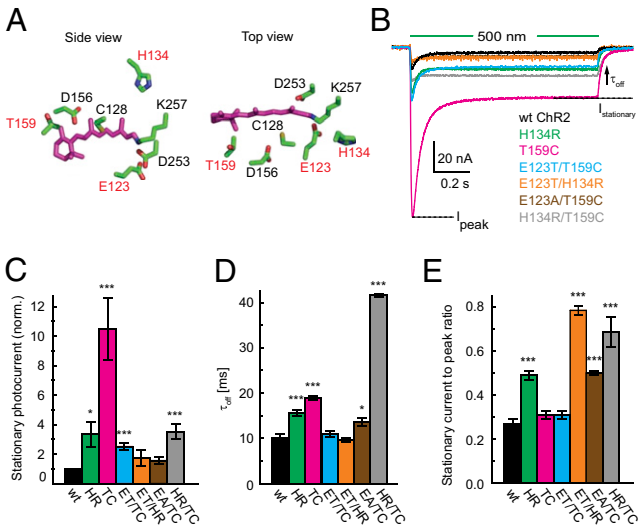

Fig. 1. Biophysical characterization of photocurrents in *Xenopus* oocytes. (*A*) Homology model of the ChR2 retinal binding pocket based on bacteriorhodopsin X-ray data (Protein Data Bank ID Code 1C3W). The chromophore is shown in magenta; residues that have been replaced in this study are labeled in red. (*B*) Typical photocurrents in oocytes excited by a 1-s light pulse (500 nm, green bar) measured at −100 mV. During light stimulation, the peak current (I_{peak}) decays to a lower stationary level ($I_{stationary}$). The off-kinetics (τ_{off}) were extracted from tail currents. (*C*) Stationary photocurrents of single and double mutants ($I_{stationary}$), normalized to the reference values of wt ChR2 (I_{wt}, black; n = 15). HR (green; n = 9), TC (magenta; n = 9), ET/TC (blue; n = 13), EA/TC (red; n = 9), and HR/TC (gray; n = 8). (*D*) Channel closure (τ_{off}) of ET/TC (blue) was as fast as wt ChR2 (black); all other tested mutants were significantly slower. (*E*) Inactivation under continuous light conditions (ratio of $I_{stationary}$ to I_{peak}) of TC and ET/TC was similar to wt ChR2. In HR, ET/HR, EA/TC, and HR/TC, inactivation was significantly reduced. ***P < 0.005; *P < 0.05.

stant of channel closure (τ_{off}) after 1 s of illumination, which was indeed significantly slowed down in HR and TC (Fig. 1*D*). In an attempt to accelerate the kinetics of TC, we mutated the counter ion at E123, a position that has been reported to accelerate channel kinetics (6). Indeed, the double mutants ET/TC and E123T/H134R (ET/HR, or "ChETA") were closing as fast as wt ChR2, whereas stationary current amplitude was still significantly enhanced in ET/TC. E123A/T159C (EA/TC) had less favorable properties than ET/TC. Finally, we tested the double mutant HR/TC, but the improvements of the single mutations were not combined, and off-kinetics was very slow. During continuous light stimulation, wt ChR2 showed strong inactivation, which can be quantified by the ratio of stationary ($I_{stationary}$) to peak current (I_{peak}; Fig. 1*E*). Inactivation of TC and ET/TC was similar to wt ChR2, whereas HR, ET/HR, EA/TC, and HR/TC showed significantly less inactivation.

Biophysical Characterization of Selected ChR2 Mutants. Because a combination of fast channel kinetics and large current amplitude is advantageous for many neurobiological applications, we decided to characterize the fastest (ET/HR, ET/TC) and high-current (HR, TC) mutants in more detail. For more precise measurements of channel kinetics, we excited the mutants by 10-ns laser flashes and measured the time to peak photocurrent (flash-to-peak). Time constants of channel closure (τ_{off}) were determined by monoexponential fit to the decay phase of the flash-induced currents at a holding potential of −50 mV. HR and TC were significantly slower than wt, whereas ET/HR and ET/TC were significantly faster (Fig. 2*A*). Interestingly, we discovered that the kinetics of HR, TC, and wt ChR2 were strongly dependent on membrane potential: At +50 mV (Fig. 2*B*), channel

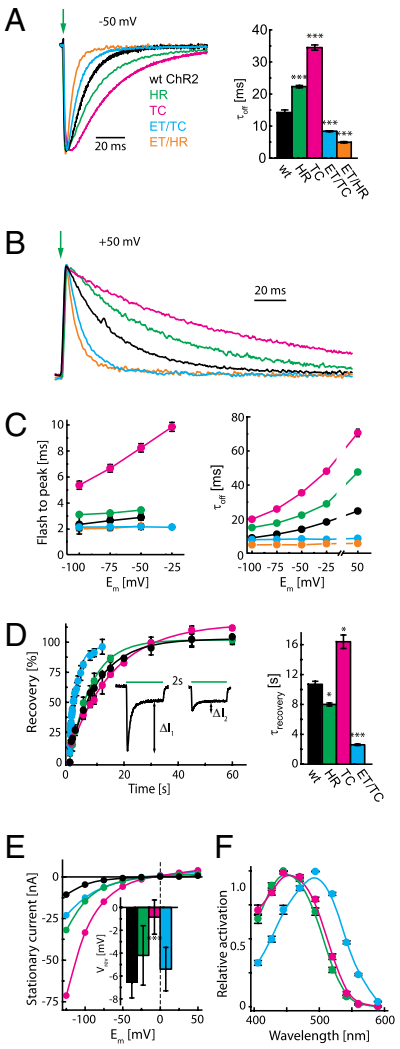

Fig. 2. Voltage-dependence of channel kinetics and spectral properties of ChR2 mutants. (*A*) Photocurrents after laser flash activation (10 ns; green arrow) measured at −50 mV, normalized to the peak. ET/HR and ET/TC were significantly faster than wt ChR2, whereas HR and TC were significantly slower.***P < 0.005. (*B*) Photocurrents after laser flash activation at +50 mV. TC, HC, and wt ChR2 slowed down considerably at this membrane potential, whereas ET/HR and ET/TC retained their fast kinetics. (*C*) To quantify the voltage-dependence of channel kinetics, flash-to-peak and τ_{off} were analyzed at different membrane potentials (n = 10 cells for each mutant). (*D*) Time-dependent recovery of peak currents (I_{peak}) was measured under physiological conditions at −75 mV in oocytes. Recovery was defined as the ratio of ΔI_2 ($I_{peak2} - I_{stationary2}$) to ΔI_1 ($I_{peak1} - I_{stationary1}$) and plotted against the interpulse interval. Recovery time constants (τ_{rec}) of HR (green; n = 3) and ET/TC (blue; n = 3) were significantly faster than wt ChR2 (black; n = 15), whereas TC (magenta; n = 3) was slower. ***P < 0.005; *P < 0.05. (*E*) IV curves show that the typical inward rectification of wt ChR2 (black) is retained in all mutants. Reversal potentials ($V_{reversal}$) were close to zero under physiological conditions (*Inset*; n = 10, 10, 12, 8). (*F*) Action spectra measured in hippocampal neurons show red-shifted wavelength optimum of ET/TC (blue curve, n = 13) relative to HR (green curve, n = 10) and TC (red curve, n = 11).

closure was two to three times slower compared with the closing speed at −100 mV (Fig. 2*C* and Tables S1 and S2). In contrast, ET/TC and ET/HR had very fast kinetics (τ_{off} = 8 and 5 ms, respectively) at all tested membrane potentials. Channel opening times were also voltage-dependent, but differences were less dramatic. We conclude that Glu-123 (mutated in E123T) not only controls absorption and kinetics of ChR2 (10), but also plays an important role in voltage sensing. For neuronal stimulation,

voltage-independent kinetics is a very desirable feature, because fast channel closure at depolarized potentials is critical to enable rapid repolarization after APs.

A further design goal was fast recovery of the peak current during repetitive stimulation (Fig. 2*D Inset*). The recovery time constant in the dark ($\tau_{recovery}$) was slightly accelerated for HR ($\tau_{recovery}$ = 8.5 vs. 10 s for wt) and slower for TC ($\tau_{recovery}$ = 16 s). In ET/TC, recovery of the peak current was remarkably fast ($\tau_{recovery}$ = 2.6 s), making it most suitable for repetitive stimulation. All tested ChR2 variants maintained the typical inward rectification of wt ChR2 with reversal potentials close to zero, suggesting that ion selectivity was not dramatically altered (Fig. 2*E*). The reversal potential of TC was slightly but significantly shifted from −6.7 mV (wt) to −0.8 mV (Fig. 2*E Inset*), pointing to enhanced Na^+ permeability.

The spectral properties of HR, TC, and ET/TC were characterized in patch-clamp recordings from cultured hippocampal neurons (*SI Methods*). Photocurrents were induced by low-intensity light pulses of different wavelengths (Fig. 2*F*). Action spectra of HR and TC were similar to wt ChR2, with the largest currents induced at 470 nm. In ET/TC, however, the optimal wavelength was red-shifted to 505 nm. Red-shifted excitation is desirable for in vivo applications because short wavelengths are strongly scattered in brain tissue.

Photocurrents in Hippocampal Slice Culture. To test the performance of TC and ET/TC in pyramidal cells, we coexpressed them with cytoplasmic red fluorescent protein (RFP) in rat hippocampal slice cultures. wt ChR2, the HR variant and the ChETA double mutant ET/HR served as references. The sparse expression pattern we obtained with particle-mediated gene transfer allowed us to identify transfected hippocampal pyramidal neurons and to target them for whole-cell recordings (Fig. 3*A*). Neurons transfected with the ChR2 variants appeared to be healthy and did not display any obvious morphological abnormalities (Fig. 3*B*). We first quantified stationary photocurrent amplitudes in response to 500-ms pulses of bright blue light (42 mW/mm^2; Fig. 3*C*). To isolate light-evoked currents, we blocked AMPA and NMDA receptor-mediated excitatory synaptic input by a mixture of 2,3-dioxo-6-nitro-1,2,3,4-tetrahydrobenzo[f]quinoxaline-7-sulfonamide (NBQX) and 3-[(*R*)-2-carboxypiperazin-4-yl]-propyl-1-phosphonic acid (CPP). Compared with photocurrents in wt ChR2 cells (967 ± 114 pA), currents in TC cells were significantly increased (1,762 ± 182 pA, $P < 0.005$). The increase in photocurrent in HR (1,312 ± 154 pA, $P = 0.102$) and ET/TC expressing cells (1,420 ± 180 pA, $P = 0.071$), due to the large variability in expression levels, was not statistically significant. ET/HR produced smaller photocurrents than wt (375 ± 56 pA, $P < 0.005$).

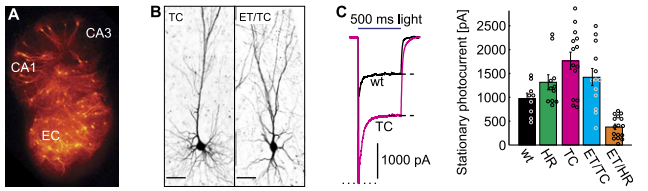

Fig. 3. Photocurrents of ChR2 variants in hippocampal pyramidal neurons. (*A*) Neurons in a sparsely transfected rat organotypic slice culture expressing TC and dimeric RFP. (*B*) Contrast-inverted two-photon images of individual transfected pyramidal neurons. (Scale bar: 50 μm.) (*C Left*) Photocurrents evoked by 500-ms blue laser illumination (42 mW/mm^2). Stationary photocurrents were quantified at the end of the stimulation pulse (dashed line) in neurons that were electrically isolated by blocking excitatory synaptic input with NBQX and dCPP. Escape APs were cropped for clarity (dotted line). (*Right*) Quantification of stationary photocurrents (n = 9, 11, 14, 13, and 16 for wt, HR, TC, ET/TC, and ET/HR, respectively). Circles depict measurements from individual cells.

AP Induction at 1–100 Hz. The large photocurrent amplitudes showed that all channelrhodopsin variants we tested were well-expressed in neurons and confirmed the photocurrent enhancement with TC that we observed in oocytes. The most common and important application of ChR2 in neurons, however, is the induction of APs with high temporal precision using brief light pulses. Hippocampal pyramidal cells transfected with wt ChR2 or HR were able to reliably follow a train of 60 bright light pulses at 40 Hz only for the first 4–7 pulses (Fig. 4*A Left*). Later during the train, they fired APs only sporadically, reflecting the transition from high peak currents to substantially lower stationary currents that is characteristic for ChR2. In contrast, neurons transfected with TC and ET/TC typically sustained firing during the entire train of 60 light pulses. Some TC-transfected neurons did produce APs of reduced amplitude early in the train, indicating depolarization block due to overly large photocurrents. At very low light levels, on the other hand, TC-transfected neurons were the only ones still responsive to the stimulus (Fig. 4*A Right*). This example might illustrate that there is no "ideal" channelrhodopsin for all applications, but experimental conditions have to be considered when choosing the "right" optogenetic tool.

To evaluate the performance of different ChR2 variants more systematically under a broad range of stimulus conditions, we stimulated transfected pyramidal cells with 2-ms light pulses at seven different frequencies (1–100 Hz). Each light pulse train was presented at four different intensities (1.9, 6.7, 23, and 42 mW/mm^2), resulting in a total of 28 different stimulus patterns for each neuron. At low stimulation frequencies (1 Hz) and high light intensities, the firing success rate (defined as the percentage of light pulses triggering at least one AP) was close to 100% for all ChR2

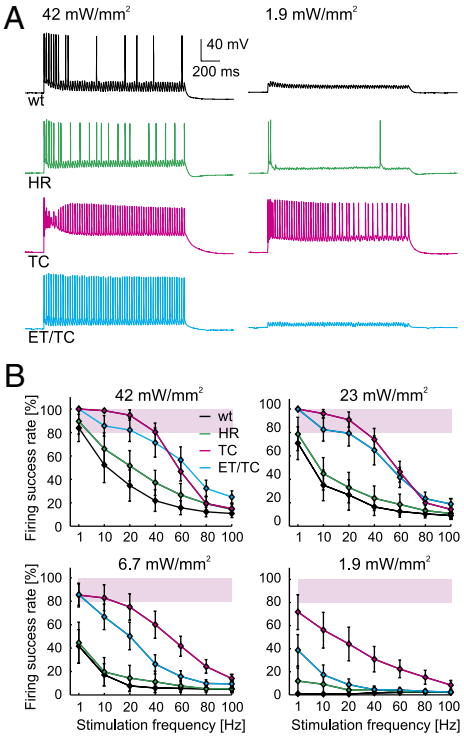

Fig. 4. Stimulation performance of TC variants at 1–100 Hz. (*A Left*) Whole-cell current-clamp recordings from pyramidal neurons stimulated with 60 brief (2 ms) light pulses at 40 Hz at high laser intensity (42 mW/mm^2). Light-evoked activity was isolated by blocking excitatory synaptic input. (*Right*) Stimulation of the same cells with low (1.9 mW/mm^2) light power. (*B*) Summary of the firing success rates from 1 to 100 Hz at different stimulation intensities (n = 9, 9, 12, and 13 for wt, HR, TC, and ET/TC, respectively). Note the high stimulation efficacy of TC and ET/TC even at low light intensities.

NEUROSCIENCE

variants. For wt ChR2 and HR, the success rate decreased rapidly with increasing stimulation frequency (Fig. 4*B*). In contrast, most cells expressing TC or ET/TC fired reliably throughout the stimulation train up to 40 Hz. As expected, the faster double mutant outperformed TC at very high frequencies (60–100 Hz) but only under bright light conditions. When lower light intensities were used for stimulation (1.9–6.7 mW/mm^2), TC had the advantage over all other mutants at all tested frequencies, recommending it for low-light applications. ET/HR-transfected pyramidal cells had success rates <5%, even under bright light conditions (n = 12 cells), consistent with the small photocurrents (Fig. 3*C*).

For some optogenetic experiments, the average spiking performance across all transfected cells might be less important than the fraction of cells that followed the light stimulus reliably. Therefore, we also analyzed firing reliability in individual neurons. Using a success rate of 80% as an arbitrary threshold for "good" performance, 45% of ET/TC neurons still performed well at 60-Hz stimulation, but only 18% of TC neurons, 11% of HR neurons, and no neuron expressing wt ChR2 (Fig. S1). Thus, for high-frequency spiking under bright light conditions, channel kinetics trumps photocurrent amplitude. At lower frequencies, both TC and ET/TC neurons could be stimulated reliably with only few neurons dropping below the 80% level. Together, these data show that TC and ET/TC outperform the commonly used H134R variant across the entire stimulus space. Specifically, the TC mutant makes it possible to spike large pyramidal cells with very dim and short light pulses, whereas all other ChR2 variants failed to induce spikes in this regime.

Precision of AP Induction. Compared with the fast Na^+ and K^+ channels activated during the AP, the on- and off-kinetics of ChR2 are relatively slow. Channelrhodopsin photocurrents can therefore outlast the AP, resulting in an after-depolarization that affects release probability at axonal boutons of ChR2-expressing neurons (12). In addition, at high expression levels, ChR2 can evoke several APs in response to a single light pulse. Spurious extra spikes compromise the precision of optogenetic AP induction, and the enhanced photocurrents combined with the slower off-kinetics we measured in TC-expressing cells suggested potential multiplet firing. Not surprisingly, in many strongly expressing TC neurons, we observed induction of doublets or triplets in response to high-intensity, 2-ms light pulses (Fig. 5*A*). In general, multiplet firing was much reduced at lower light intensities (Fig. 5*A Right*) and largely absent at frequencies of 10 Hz or higher (Fig. 5*B*). Even in TC-expressing neurons, only the first light pulses in a long train could trigger sufficiently large currents to induce more than one spike, due to the transition from peak to stationary photocurrents.

A second consequence of large photocurrents with slow off-rates is buildup of plateau depolarizations at high stimulation frequencies, because cells cannot repolarize sufficiently between individual stimulation pulses (Fig. 5*C*). At frequencies of 40 Hz or more and high light intensity, neurons expressing the high current versions HR and TC displayed significantly stronger plateau depolarization than wt ChR2 (Fig. 5*C*). We were initially surprised about the very small plateau depolarization recorded in ET/TC expressing neurons, despite their large photocurrents. Further analysis showed that the amplitude of plateau depolarization at 100 Hz is highly correlated with the product of photocurrent amplitude and off time constant (R = 0.986; Fig. 5*D*), indicating that the biophysical properties of the mutants fully explain the generation of plateau potentials at high frequencies.

Together, these data suggest that TC is best suited for optical stimulation at low light intensities or low expression levels, whereas at moderate and high light intensities, ET/TC allows single AP induction with high accuracy because of its accelerated kinetics at all membrane potentials.

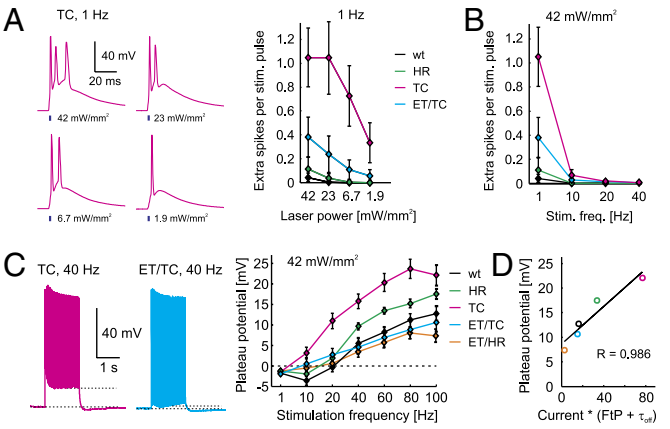

Fig. 5. Precision of single AP induction. (*A Left*) With high stimulation light intensity, TC often evoked several spikes in response to a single 2-ms light pulse during 1-Hz stimulation. (*Right*) Multiplet firing is observed mostly with TC and is reduced at lower stimulation intensity. (*B*) Multiplet firing is largely restricted to 1-Hz stimulation and rarely occurs at higher stimulation frequencies. (*C Left*) Example spike trains from neurons expressing TC or ET/TC stimulated with 60 2-ms pulses at 40 Hz with 42 mW/mm^2 light intensity. Plateau potentials were measured between baseline and the minimal membrane depolarization during the last 500 ms of the stimulation train (dashed lines). (*Right*) Summary of plateau potentials for 1- to 100-Hz stimulation (n = 9, 11, 14, 13, and 12 for wt, HR, TC, ET/TC, and ET/HR, respectively). (*D*) Plateau depolarization at 100 Hz was highly correlated with the product of photocurrent amplitude and channel closing speed.

Discussion

Previous attempts to improve ChR2 have yielded faster mutants that produced smaller currents and mutants with large currents that were slower than wt ChR2 (Fig. 6). The anticorrelation between photocurrent amplitude and kinetics is not surprising, because thermodynamic stabilization of the open state slows down channel closure, which increases the charge transfer through single channels during a single photocycle.

Here we introduce two previously undescribed ChR2 mutants that are particularly suitable for optogenetic stimulation of neurons. The ET/TC double mutant has an accelerated photocycle, which is apparent from the fast rise and decay of the photocurrent and, once in the dark, the rapid recovery to the dark state (Fig. 2). In addition, ET/TC produces larger stationary photocurrents while maintaining the ion selectivity of wt ChR2, as indicated by the unchanged reversal potential (Fig. 2*E*). The action spectrum is red-shifted by ~35 nm, which should be helpful for in vivo applications where the strong scattering of blue light can be a problem. Furthermore, the red-shifted absorption makes it possible to activate ET/TC at 530 nm, where the recently discov-

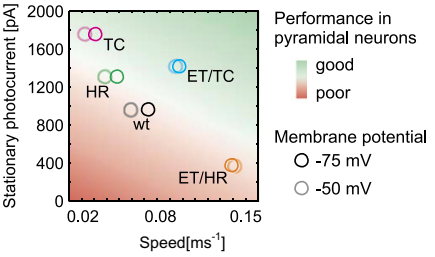

Fig. 6. Evaluation of different ChR2 variants for use in pyramidal neurons. Photocurrent amplitude (same data as Fig. 3*C*) and channel speed, defined as (flash to peak + τ_{off})$^{-1}$ (same data as Fig. 2*C*) determine the performance in neurons. Bright circles, kinetics at −75 mV; pale circles, at −50 mV. The ideal ChR should gate large currents with rapid kinetics (green shaded corner).

ered photoactivated adenylyl cyclases (13, 14) do not absorb. Both membrane potential and intracellular cAMP levels can therefore be controlled independently by blue and green light, respectively. When ET/TC was expressed in pyramidal cells, spikes were induced with higher fidelity across a wide range of light intensities and stimulation frequencies. We attribute the greatly improved performance of ET/TC in neurons largely to its accelerated and voltage-independent kinetics, allowing rapid membrane repolarization following each AP. In contrast, during high-frequency stimulation of wt ChR2 and HR, a plateau depolarization develops (Fig. 5*C*), leading to Na^+ channel inactivation. In summary, ET/TC breaks the amplitude vs. speed tradeoff seen in previous ChR2 variants (Fig. 6) and will outperform wt ChR2 and the HR variant for all experimental conditions.

The second mutant we present in this work is the TC single mutant, which generated extremely large stationary photocurrents of up to 3 nA in pyramidal cells. When driven by the synapsin 1 promoter, the currents were large enough to trigger multiple spikes in response to bright 2-ms light pulses and could even lead to depolarization block. We also demonstrated that TC could still induce spikes at very low light intensities where all other ChR2 variants produced only subthreshold depolarizations. The low light levels needed to stimulate TC-expressing neurons greatly reduce the risk of phototoxicity, especially in chronic stimulation experiments (15). Large photocurrents may also be helpful when weaker and more specific promoters have to be used, for example, to activate genetically defined subsets of neurons.

Of note was the different magnitude of current enhancement by TC in oocytes (10-fold over wt) and neurons (2-fold over wt). Very likely, the TC mutation improved protein expression, folding, or targeting to the plasma membrane, as well as single channel properties. We do not fully understand the mechanism of the current enhancement, but noted the slightly positively shifted reversal potential of TC, pointing to enhanced Na^+ conductance (16). Despite the very large currents they generated, the expression and activation of TC and ET/TC did not seem to cause any toxic effects in oocytes or in neurons, as strongly expressing cells were morphologically and functionally indistinguishable from weakly expressing cells. For both mutants, expression levels (as estimated by photocurrent amplitude) were not correlated with holding current or input resistance (Fig. S2).

With respect to rational molecule design, it was interesting to see that the kinetics and the current amplitude produced by the ET/TC double mutant were somewhere between the properties of the individual ET and TC mutations, but, by fortunate coincidence, the spectral properties of ET were fully retained (6). We conclude that individual beneficial mutations of ChR2 can be combined to some extent in a module-like fashion, but careful assessment of the properties of multiple mutants will always be necessary. What would be important design goals for the future? Our data suggest that we are now in a situation where photocurrent amplitudes are no longer limiting stimulation performance (Fig. S2). To further improve the reliability of optogenetic stimulation at high frequencies, light-gated channels with even faster kinetics would be required that completely eliminate plateau potentials while still gating very large photocurrents. As we have shown previously, APs triggered by wt ChR2 are associated with an increased transmitter release probability, most likely due to the relatively long duration of the light-induced current (12). Ideally, photocurrent amplitude would also be constant during continuous or repeated illumination, such that reliability and precision of AP induction does not depend any more on the history of light stimulation. Lastly, a further red shift of the absorption spectrum would be welcome, too.

In conclusion, for stimulation of large pyramidal cells with minimal light intensities or deep within neuronal tissue, we recommend the TC single variant, because it greatly increases the light sensitivity of transfected neurons. For all other experimental conditions, ET/TC is the most powerful tool because it combines rapid kinetics with large photocurrents and thereby dramatically improves the reliability of high-frequency stimulation.

Methods

Homology Model. ChR2 sequence AF 461397 was aligned to the dark-state structure of bacteriorhodopsin (Protein Data Bank ID Code 1C3W; ref. 11) with the Swiss-PdbViewer, and the ChR2 homology model was generated by the automated protein-modeling server SWISS-MODEL (17).

Oocyte Preparation. Amino acid replacement was realized by site-directed mutagenesis (QuikChange, Agilent Technologies) of the pGEMHE-ChR2 plasmid. We used a shortened ChR2 sequence (residues 1–315) as template for mRNA synthesis by T7 RNA polymerase (mMessage mMachine, Ambion). Oocytes from *Xenopus laevis* were injected with 20 ng of mRNA and stored for 3–7 d in the dark at 18 °C in Ringer's solution (96 mM NaCl, 5 mM KCl, 1.8 mM $CaCl_2$, 1 mM $MgCl_2$, 5 mM Mops·NaOH, 50 units/Ll penicillin, and 0.05 mg/mL streptomycin, pH 7.5).

Oocyte Photostimulation and Recording. Two-electrode voltage clamp data were recorded with a Turbo Tec-05× (NPI Electronic) or a GeneClamp 500 (Molecular Devices) amplifier in a solution containing (in mM) 100 NaCl, 1 $MgCl_2$, 0.1 $CaCl_2$, and 5 Mops·NaOH, pH 7.5. Continuous light was provided by a 75-W Xenon lamp (Jena Instruments) and delivered to the oocytes via a 3-mm light guide. The light passed through a 500 ± 25-nm broadband filter (Balzers) and provided 3.4 mW/cm^2 light intensity. For fast kinetics measurements, we applied 10-ns laser flashes at 470 and 500 nm with an adjustable Rainbow OPO (Opotek) pumped by Brilliant b Nd:YAG-Laser (Quantel). Mutants and wt ChR2 were always measured on the same day because protein expression and photocurrent amplitudes increased over time. Data were analyzed with Clampfit 10 (Molecular Devices) and OriginPro 8G (OriginLab Corporation).

Slice Culture Preparation and Transfection. Hippocampal slice cultures from Wistar rats were prepared at postnatal day 4–5 as described (18). After 7 d in culture, we used a Helios gene gun (Bio-Rad) to cotransfect individual cells with DNA encoding a specific ChR2 variant and soluble tdimer2 (19), each subcloned into a neuron-specific expression vector under control of the human synapsin-1 promoter. For gene-gun transfection, 5 mg of 1.6-μm gold bullets (Bio-Rad) was coated with a total of 8 mg of DNA at a ChR2:tdimer2 molar ratio of 6:1. Point mutations (H134R, T159C, E123T) were introduced into wt ChR2 by site-directed mutagenesis (QuikChange, Agilent Technologies).

Slice Culture Photostimulation and Recording. The recording setup was based on a BX-51 microscope equipped with a LUMPlan 60× 0.9NA water immersion objective (Olympus) and a cooled CCD camera (Sensicam QE). A 473-nm laser (Oxxius) controlled by an acousto-optic modulator (AA Opto-Electronic) was fiber-coupled to the microscope. For patch-clamp recordings, we used a MultiClamp 700B amplifier (Molecular Devices) controlled by the Matlab-based software package Ephus (20). Experiments were conducted at 29–31 °C 1–3 wk after transfection in artificial cerebrospinal fluid containing (in mM) 127 NaCl, 2.5 KCl, 2 $CaCl_2$, 1 $MgCl_2$, 25 $NaHCO_3$, 25 D-glucose, 1.25 NaH_2PO_4, 0.01 NBQX, and 0.01 dCPP, pH 7.3. Patch-clamp electrodes were filled with (in mM) 135 K-gluconate, 4 $MgCl_2$, 4 Na_2-ATP, 0.4 Na-GTP, 10 Na_2-phosphocreatine, 3 ascorbate, and 10 Hepes (pH 7.2). In current-clamp experiments, a small holding current was injected to hold the cells at −60 mV. Voltage-clamp experiments were performed at −65 mV holding potential. For quantification, APs were automatically detected as brief membrane potential excursions with minimal amplitude of 40 mV. Firing success rate was defined as the percentage of light pulses evoking at least one AP. Extra spikes fired in response to a single light pulse were summed up for each pulse train and divided by the number of light pulses that successfully induced AP firing. Plateau potentials were defined as the difference between baseline membrane potential and the most negative potential during the last 500 ms of the stimulation train.

Statistical Analysis. Numerical values are given as mean ± SEM. We used Student *t* test (two-tailed) to assign statistical significance: $P < 0.005$ (***), $P < 0.01$ (**), $P < 0.05$ (*).

ACKNOWLEDGMENTS. We thank Daniela Gerosa Erni and Maila Reh for excellent technical support. A.B. is supported by the Leibniz Graduate School for Molecular Biophysics and a European Molecular Biology Organization short-term fellowship. P.S. and T.G.O. were supported by the Novartis Research Foundation and the Gebert Rüf Foundation. P.H. was supported by the German Research foundation, DFG (HE 3824/9-3 &18-1).

1. Nagel G, et al. (2003) Channelrhodopsin-2, a directly light-gated cation-selective membrane channel. *Proc Natl Acad Sci USA* 100:13940–13945.
2. Boyden ES, Zhang F, Bamberg E, Nagel G, Deisseroth K (2005) Millisecond-timescale, genetically targeted optical control of neural activity. *Nat Neurosci* 8:1263–1268.
3. Atasoy D, Aponte Y, Su HH, Sternson SM (2008) A FLEX switch targets Channelrhodopsin-2 to multiple cell types for imaging and long-range circuit mapping. *J Neurosci* 28: 7025–7030.
4. Kuhlman SJ, Huang ZJ (2008) High-resolution labeling and functional manipulation of specific neuron types in mouse brain by Cre-activated viral gene expression. *PLoS One* 3:e2005.
5. Nagel G, et al. (2005) Light activation of channelrhodopsin-2 in excitable cells of Caenorhabditis elegans triggers rapid behavioral responses. *Curr Biol* 15:2279–2284.
6. Gunaydin LA, et al. (2010) Ultrafast optogenetic control. *Nat Neurosci* 13:387–392.
7. Martina M, Schultz JH, Ehmke H, Monyer H, Jonas P (1998) Functional and molecular differences between voltage-gated K+ channels of fast-spiking interneurons and pyramidal neurons of rat hippocampus. *J Neurosci* 18:8111–8125.
8. Berndt A, Yizhar O, Gunaydin LA, Hegemann P, Deisseroth K (2009) Bi-stable neural state switches. *Nat Neurosci* 12:229–234.
9. Schoenenberger P, Gerosa D, Oertner TG (2009) Temporal control of immediate early gene induction by light. *PLoS ONE* 4:e8185.
10. Hegemann P, Möglich A (2011) Channelrhodopsin engineering and exploration of new optogenetic tools. *Nat Methods* 8:39–42.
11. Luecke H, Schobert B, Richter HT, Cartailler JP, Lanyi JK (1999) Structure of bacteriorhodopsin at 1.55 A resolution. *J Mol Biol* 291:899–911.
12. Zhang YP, Oertner TG (2007) Optical induction of synaptic plasticity using a light-sensitive channel. *Nat Methods* 4:139–141.
13. Stierl M, et al. (2011) Light modulation of cellular cAMP by a small bacterial photoactivated adenylyl cyclase, bPAC, of the soil bacterium Beggiatoa. *J Biol Chem* 286:1181–1188.
14. Schröder-Lang S, et al. (2007) Fast manipulation of cellular cAMP level by light in vivo. *Nat Methods* 4:39–42.
15. Godley BF, et al. (2005) Blue light induces mitochondrial DNA damage and free radical production in epithelial cells. *J Biol Chem* 280:21061–21066.
16. Berndt A, Prigge M, Gradmann D, Hegemann P (2010) Two open states with progressive proton selectivities in the branched channelrhodopsin-2 photocycle. *Biophys J* 98:753–761.
17. Guex N, Peitsch MC (1997) SWISS-MODEL and the Swiss-PdbViewer: an environment for comparative protein modeling. *Electrophoresis* 18:2714–2723.
18. Stoppini L, Buchs PA, Muller D (1991) A simple method for organotypic cultures of nervous tissue. *J Neurosci Methods* 37:173–182.
19. Campbell RE, et al. (2002) A monomeric red fluorescent protein. *Proc Natl Acad Sci USA* 99:7877–7882.
20. Suter BA, et al. (2010) Ephus: Multipurpose data acquisition software for neuroscience experiments. *Front Neurosci* 4:53–61.

Supporting Information

Berndt et al. 10.1073/pnas.1017210108

SI Methods

Action Spectra Measurements. Action spectra were measured in dissociated hippocampal neurons. Mammalian codon-optimized ChR2(H134R), ChR2(T159C), and ChR2(E123T/T159C) was cloned into a lentiviral backbone with CaMKIIα promoter (FCK) and fused in-frame with YFP at the C terminus to enable visualization of expressing neurons. Primary hippocampal cultures were prepared from P0 Sprague-Dawley rat pups, transfected at 4 d in vitro with 2 μg of DNA per coverslip, and recorded 4–6 d later. Recordings were performed at room temperature in Tyrode's solution containing (in mM) 125 NaCl, 2 KCl, 3 $CaCl_2$, 1 $MgCl_2$, 30 glucose, and 25 Hepes (pH 7.3) in the presence of bath-applied TTX (1 μM) and intracellular QX-314 chloride (1 mM) to prevent escaped spikes. The intracellular solution contained (in mM) 130 K-gluconate, 10 KCl, 10 EGTA, 2 $MgCl_2$, and 10 Hepes (pH 7.0). Light pulses were delivered through a 40× water-immersion objective. Light from a 300-W DG-4 lamp (Sutter Instruments) was passed through bandpass and neutral density filters to generate closely matched power densities. Action spectra were determined by measuring the peak photocurrent in response to 3-ms subsaturating light pulses (range: 4.4–6.3 mW/mm^2). Measured photocurrents were scaled to correct for the small power density differences at different wavelengths, then normalized to action spectrum peak within cells followed by averaging across cells.

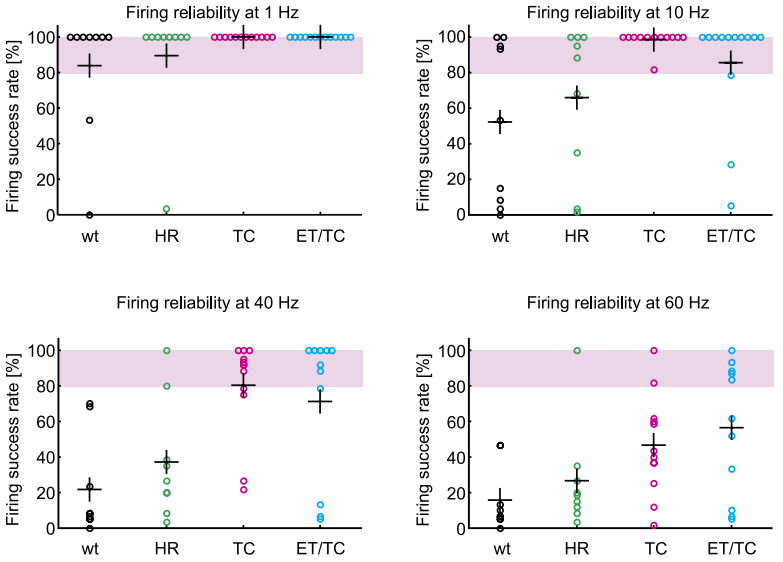

Fig. S1. Firing reliability in individual pyramidal neurons. Pyramidal neurons were stimulated with 60 light pulses of 2-ms duration at 42 mW/mm^2 laser power. Crosses indicate averages. Note that with 40-Hz stimulation, TC and ET/TC drive firing with high reliability between 80% and 100% in more than half of the neurons. At a stimulation frequency of 60 Hz, 5/11 cells expressing ET/TC still sustained firing with >80% reliability.

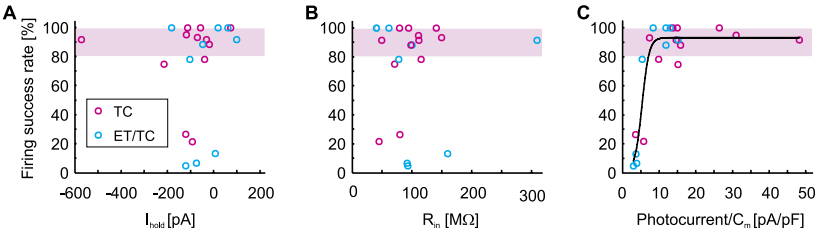

Fig. S2. Analysis of cell viability and factors governing firing success rate. For individual neurons expressing TC or ET/TC, the firing success rate during a 40-Hz stimulation train with 42 mW/mm^2 light intensity is plotted against cellular parameters that were determined in voltage-clamp experiments. (*A*) The firing success rate in current clamp experiments is not correlated with the holding current required to clamp the cells at −65 mV (R = 0.03, P = 0.89). Well firing neurons (pink bar) are found in the entire range of holding currents. (*B*) The firing success rate is not correlated with input impedance (R = 0.04, P = 0.86). (*C*) The firing success rate is best predicted by the photocurrent amplitude in relation to a neuron's membrane capacitance. The black line represents a sigmoidal fit.

Table S1. Voltage dependence of channel kinetics: Flash-to-peak

Holding pot	−100 mV	−75 mV	−50 mV	−25 mV
wt ChR2	2.34 ± 0.08	2.64 ± 0.11	2.90 ± 0.10	n. d.
HR	***3.04 ± 0.03	***3.32 ± 0.03	***3.45 ± 0.07	n. d.
TC	***5.10 ± 0.21	***6.42 ± 0.19	***7.95 ± 0.17	9.85 ± 0.41
ET/TC	2.15 ± 0.13	*2.17 ± 0.13	***2.19 ± 0.12	2.16 ± 0.16
ET/HR	2.02 ± 0.18	*2.06 ± 0.18	***2.08 ± 0.16	n. d.

Values are in milliseconds. n.d., no data. ***$P < 0.005$; *$P < 0.05$.

Table S2. Voltage dependence of channel kinetics: Off time constant

Holding pot	−100 mV	−75 mV	−50 mV	−25 mV	+50 mV
wt ChR2	9.01 ± 0.29	11.10 ± 0.47	14.22 ± 0.59	18.83 ± 0.59	24.67 ± 1.09
HR	***15.02 ± 0.21	***17.56 ± 0.21	***22.31 ± 0.37	***28.89 ± 0.59	***47.61 ± 1.11
TC	***19.92 ± 0.21	***25.92 ± 0.49	***35.36 ± 0.49	***47.02 ± 1.37	***71.88 ± 2.03
ET/TC	***7.89 ± 0.15	***8.11 ± 0.13	***8.38 ± 0.12	***8.12 ± 0.16	***8.70 ± 0.26
ET/HR	***4.89 ± 0.11	***4.98 ± 0.14	***4.91 ± 0.27	***5.57 ± 1.11	***5.71 ± 0.36

Values are in milliseconds. ***$P < 0.005$.